



Data-Based Energy Demand Prediction for Hybrid Electrical Vehicles

Daniel Fink¹ · Oliver Maas¹ · Daniel Herda¹ · Zygimantas Ziaukas¹ · Christoph Schweers² · Ahmed Trabelsi² · Hans-Georg Jacob¹

Received: 29 August 2022 / Accepted: 5 November 2023
© The Author(s) 2024

Abstract

To achieve a resource-efficient automotive traffic, modern driver assistance systems minimize the vehicle's energy demand through speed optimization algorithms. Based on predictive route data, the required energy for upcoming operation points has to be determined. This paper presents a method to predict the energy demand of a hybrid electrical vehicle. Within this method, data-based approaches, such as neural networks, Gaussian processes, and look-up tables, are applied and assessed regarding their ability to predict the behavior of separate powertrain parts. The applied approaches are trained using measured data of a test vehicle. As a result, for every separate powertrain part, the best-suited data-based approach is selected to obtain an optimal energy demand prediction method. On a validation data set, this method is able to predict the transmission ratio of the gearbox causing a rmse of 0.426. The combustion engine's torque prediction results in an rmse of 19.01 Nm and the electric motor torque prediction to 19.11 Nm. The root mean square error of the motor voltage results to 1.211 V.

Keywords Systems modeling · Energy demand prediction · Hybrid electrical vehicles

Introduction

Sustainability and resource efficiency are key challenges to reducing emissions and global warming. To achieve this, manufacturers aim to develop vehicles with the lowest possible energy consumption. The driver's behavior plays a significant role in the vehicle's energy demand [1]. Hence, increasing vehicle control automation, while maintaining the drivers preferences in driving dynamics, offers a high potential to reduce energy demand [2, 3]. Energy-efficient driving automation is part of current research [4]. A well-established procedure is to plan and optimize the vehicle's speed trajectory for the upcoming route section. A common approach is to use a dynamic programming (DP) algorithm for the optimization process [5]. Within this process, an energy model

of the vehicle is used to predict the energy demand based on predictive route data.

State of the Art and Related Work

The application of a DP-based optimization approach within a risk-sensitive nonlinear model predictive controller is shown in [6]. This increases energy efficiency by 21% for an electric vehicle. An approach to predict the energy demand of hybrid electric vehicles with a series drive configuration is presented by [7]. For more complex hybrid drive concepts, the literature mainly provides research works that are based on energy management strategies [8, 9]. These strategies are not suited to be applied within route data-based speed-optimizing algorithms. They rely on adjusting the torque distribution between the combustion engine and electric motor based on measured internal states of both engines. The prediction of all internal engine states required for these strategies is very challenging and would result in high model complexities and enormous computing effort [10]. Addressing this problem, [11] presented a hybrid vehicle energy consumption model which is capable of determining the consumed amount of fuel. However, the required energy demand of the electric drive train part is not considered.

This article is part of the topical collection "Vehicle Technology and Intelligent Transport Systems" guest-edited by Oleg Gusikhin and Markus Helfert.

✉ Daniel Fink
daniel.fink@imes.uni-hannover.de

¹ Institute of Mechatronic Systems, Leibniz University Hanover, An der Universität 1, Garbsen 30823, Niedersachsen, Germany

² IAV GmbH, Berlin, Germany

Previous Work on Energy Demand Prediction

In [12], we presented a method to predict the energy demand of a hybrid electric vehicle, in which the electric and combustion energy demand is predicted separately. It is based on modeling the behavior of the separate drive train components and can be used within speed optimization algorithms for driver assistance systems. For this purpose, a solution space with discrete vehicle states is formed. A vehicle state k within this solution space is defined by the vehicle speed v_k , the state of charge (SOC) $s_{c,k}$, the geographical height h_k and route position from which the distance Δd_k between to states can be derived. To optimize the vehicle's speed, every state transition is evaluated by a cost function in which the presented energy demand prediction method is applied. Figure 1 illustrates the structure of the existing energy demand prediction method which can be described as follows: the required torque for a state transition is determined by the height and speed differences as well as by the route distance to overcome, using a longitudinal vehicle model [13]. In parallel hybrid electric powertrains, the torque of the two engines cannot be derived directly from the required wheel torque. This torque and the drive shaft speed rely on the behavior of the gearbox as well as on the torque distribution

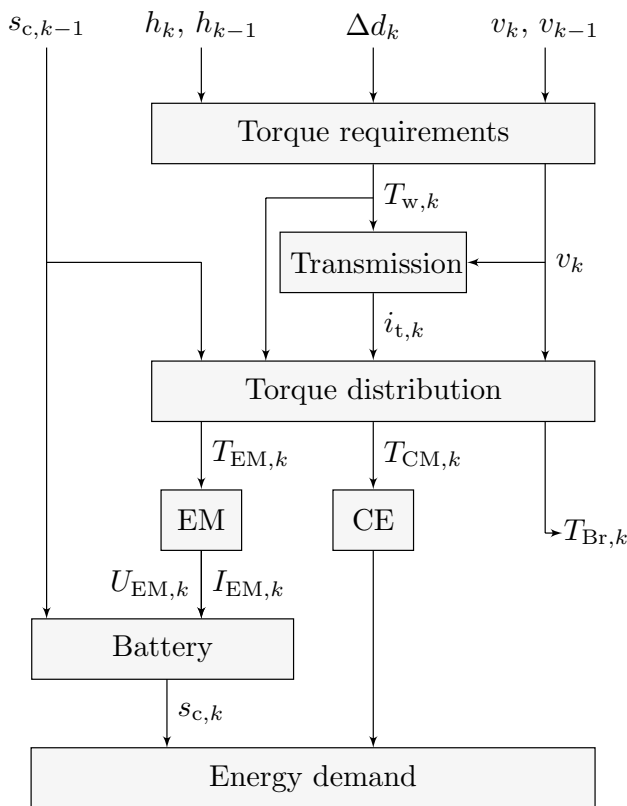


Fig. 1 Structure of the prediction approach [12]

mechanism. With the torque of the electric motor $T_{EM,k}$ and the torque of the combustion engine $T_{CE,k}$ the energy demand for the combustion engine and the required electric power of the electric motor can be determined considering the drive shaft speed. From the estimated SOC $s_{c,k}$ the energy demand of the electric powertrain can be derived. The sum of the combustion and electrical energy consumption results in the total energy demand. Using this method to predict the energy demand, a real-time capable optimization process is obtained, that can be applied online on a vehicle's control unit, as shown in [14].

However, the computing resources of a vehicle's control unit are limited. Therefore, the energy demand prediction method within the optimization algorithm mainly relies on identified lookup tables when estimating the behavior of the powertrain components.

Contribution in this Paper

In this paper, we aim to improve the energy demand prediction model independently from the in-vehicle computational constraints, for a wider range of applications, e.g. for offline energy-related route assessments in navigation algorithms. Therefore, we present data-based approaches to predict the behavior of the separate drive train parts. To the best of the authors' knowledge, these approaches have not been applied and combined for this purpose. In particular, we investigate on the prediction of the gearbox and torque distribution behavior as well as the motor voltage, as these predictions cause the largest errors within the existing method. We compare feed-forward neural networks and Gaussian processes with a lookup table-based prediction, presented in [12]. Using measured CAN data, all different prediction approaches are validated for a Volkswagen Golf VII GTE.

The paper is organized as follows: the next section gives a short summary on the existing energy demand prediction method, presented in [12], followed by the data-based approaches to be investigated for the prediction of separate drive train components. In the penultimate section, the prediction results of the different approaches are evaluated, regarding the prediction accuracy and computational complexity. Finally, the results are concluded.

Data-Based Prediction Approaches

In [12], the prediction of the transmission behavior, the torque distribution and the motor voltage show the highest error margin. In this chapter, we propose further data-based approaches to estimate the behavior of the corresponding powertrain parts, aiming to increase the accuracy of the energy demand prediction.

Transmission Estimation

The dual-clutch transmission is a main element in the prediction process, as the operation points of the combustion engine and the electric motor directly depend on its behavior. To model the gear selection process, the transmission factor $i_{t,k}^*$ is estimated depending on the vehicle speed \bar{v}_k^* and the wheel torque $T_{w,k}$ for every operation point, using weighted basis functions Φ_i and Φ_j , as described in [15]:

$$i_{t,k}(T_{w,k}, \bar{v}_k) = \sum_{i=1}^{M_t} \sum_{j=1}^{N_t} w_{t,i,j} \Phi_i(T_{w,k}, \xi_i) \Phi_j(\bar{v}_k, \eta_j). \tag{1}$$

A basis functions Φ_q is defined to be a linear function that equals 1 at a grid point c_q while it is 0 at all other grid points, as declared by

$$\Phi_q(u, \mathbf{c}) = \begin{cases} \frac{u-c_{i-1}}{c_i-c_{i-1}}, & \text{if } c_{i-1} \leq u \leq c_i \\ \frac{c_{i+1}-u}{c_{i+1}-c_i}, & \text{if } c_i < u \leq c_{i+1} \\ 0, & \text{otherwise.} \end{cases} \tag{2}$$

The real transmission factor can be calculated according to the measured vehicle speed \bar{v}_k^* and drive shaft speed $n_{d,k}^*$ by

$$i_{t,k}^* = \frac{n_{d,k}^*}{n_{w,k}} = \frac{2 \cdot \pi \cdot r_d \cdot n_{d,k}^*}{60 \cdot v_k^*}, \tag{3}$$

which is used to determine the optimal set of weights, by

$$w_{t,opt} = \arg \min_w \frac{1}{L} \sum_{k=1}^L (i_{t,k} - i_{t,k}^*)^2. \tag{4}$$

To further improve the model, we examined additional inputs. One key aspect of the switching strategy of the transmission is the accelerator pedal. The pedal’s position signal is used in the transmission control unit to adapt the shift strategy. However, as the position of the accelerator pedal cannot be used in the energy demand prediction model, we use the vehicles acceleration \bar{a}_k as an addition input value. This leads to the expansion of equation (1) by the acceleration basis function Φ_l , changing the transmission factor estimation to

$$i_{t,k}(T_{w,k}, \bar{v}_k, \bar{a}_k) = \sum_{i=1}^{M_t} \sum_{j=1}^{N_t} \sum_{l=1}^{O_t} w_{t,i,j,l} \Phi_i(T_{w,k}, \xi_i) \Phi_j(\bar{v}_k, \eta_j) \Phi_l(\bar{a}_k, \zeta_l). \tag{5}$$

We defined the grid \mathbf{c} to consist of $M_t = 23$ grid points of ξ_i for the drive wheel torque T_w , $N_t = 21$ grid points η_j for the vehicle speed \bar{v}_k^* and $O_t = 7$ grid points of ζ_l . Finally the new set of weights $w_{t,opt}$ is calculated according to equation (4).

Torque Distribution

The torque distribution determines the composition of the required total drive torque. A complex control algorithm assigns the torque to the corresponding drive or to the braking system depending on the driving situation. While deceleration the required torque is applied by a combination of the braking system and the recuperative electric motor. During driving stage the required drive shaft torque is provided by the electric motor and the combustion engine.

In [12], this behavior is modeled, by separately considering driving state and deceleration state. The deceleration state is defined by a negative total drive shaft torque $T_{t,k}$, in which the electric motor torque $T_{EM,k}$ can be estimated with regard to the state of charge $s_{c,k}$, using

$$T_{EM,k}(T_{t,k}, s_{c,k}) = \sum_{i=1}^{M_{EM}} \sum_{j=1}^{N_{EM}} w_{EM,i,j} \Phi_i(T_{t,k}, \xi_i) \Phi_j(s_{c,k}, \eta_j). \tag{6}$$

To model the torque distribution during the driving state, a distribution ratio r_k between the torque of the combustion engine $T_{CE,k}$ and electric motor torque $T_{EM,k}$ is introduced. The distribution ratio r_k is used to predict the torque applied by both power units with regard to the previous SOC $s_{c,k}$, the total drive shaft torque $T_{t,k}$ and the vehicle speed \bar{v}_k .

This approach indicates a reasonable fit on the overall distribution behavior. However, the estimated electric motor torque deviates from the measurements during the driving state when the combustion engine is running. In these phases the electric motor applies a negative torque on the driveshaft while the combustion engine provides the requested torque and an additional torque corresponding to the electric motor torque. This is called load point adjustment, because the load point of the engine is shifted through the additional electric motor torque. While the measurements show a negative electric motor torque, the torque distribution model often predicts no torque or a positive one for the electric motor. To include this behavior in the prediction model, we introduce a new approach for the driving state. The distribution factor r_k is defined as

$$r_k = \frac{T_{CE,k}}{T_{t,k}}, \tag{7}$$

and predicted depending on the total drive shaft torque $T_{t,k}$, the vehicle velocity \bar{v}_k^* and the state of charge $s_{c,k}$, as shown in [12].

Instead of estimating the distribution factor based upon weighted basis function, a feed-forward neural network as introduced by [15] is used. The feed-forward neural network uses a fully connected, 2 layered structure with 95 neurons for the first hidden layer and 40 neurons for the second

hidden layer. For the activation function of the neurons, a sigmoid function is chosen.

Neural networks are structured in different category's, each having their own field of application. They can be separated into feed forward neural networks or multi-layer perceptron networks [15], convolution neural networks and recurrent neural networks. Due to the optimization process we can only use data from a single time step. Since convolution neural networks use time series data to compute the convolution and recurrent neural networks save previous hidden layer states [16], these neural networks are not feasible for the application in the optimization process.

Assuming that the load point adjustments torque depends on the already applied engine torque, a load point ratio $r_{lpa,k}$ is defined as

$$r_{lpa,k} = \frac{T_{EM,k}}{T_{CE,k}}. \tag{8}$$

To integrate the load point adjustment into the engine torque prediction, a separate feed-forward neural network is trained upon r_{lpa} , using a fully connected, 2 layered structure with 50 neurons in the first layer and 40 neurons in the second layer. The neural network uses a sigmoid as activation function. Since a torque distribution factor above 1 would also act as load point adjustment, r_k has to be limited at 1. Therefore, the combustion engine torque is predicted as follows:

$$T_{CE,k} = \begin{cases} r_k(T_{t,k}, \bar{v}_k, s_{c,k})T_{t,k}, & \text{if } r_k < 1 \\ (1 - r_{lpa})(T_{t,k}, \bar{v}_k, s_{c,k})T_{t,k}, & \text{if } r_k \geq 1. \end{cases} \tag{9}$$

According to the assumption that the total drive shaft torque is always fully distributed between the combustion engine and the electric motor, the electric motor torque can be estimated as

$$T_{EM,k} = T_{t,k} - T_{CE,k}. \tag{10}$$

Motor Voltage

The motor voltage is a key variable to predict the state of charge. The previous approach, based on a polynomial equation, led to a significant deviation. In [12], the polynomial equation to predict the motor voltage is proposed as follows:

$$U_{EM,k}(s_{c,k-1}, T_{EM,k}) = p_{U_{EM},1} + p_{U_{EM},2} \cdot s_{c,k-1}^2 + p_{U_{EM},3} \cdot s_{c,k-1} + p_{U_{EM},4} \cdot T_{EM,k}^2 + p_{U_{EM},5} \cdot T_{EM,k}. \tag{11}$$

Using a least square algorithm, the error minimizing parameter set $p_{U_{EM}}$ was found, based on measured motor voltage values of the identification data.

In this work, we introduce a Gaussian process regression model (GPR) [17], which is used to predict the motor voltage U_{EM} based on the electric motor's torque $T_{EM,k}$, rotational speed $n_{EM,k}$ and on the current SOC $s_{c,k}$ of the battery. For training the GPR the identification data set shown in [12] was used. A GPR model predicts the value of the response variable y_{new} , given the new input vector x_{new} , and the training data. A linear regression model is of the form:

$$y = x^T \beta + \epsilon, \tag{12}$$

where $\epsilon \sim N(0, \sigma^2)$. The error variance σ^2 and the coefficients β are estimated form the identification data. The response is explained by latent variables, $f(x_i), i = 1, 2, \dots, n$, and explicit basis functions h . The latent variables are not directly observed but are inferred through a Gaussian process (GP). The basis function projects the inputs x into a p -dimensional feature space.

A GP is defined by its covariance function $k(x, x')$ and its mean function $m(x)$. If $\{f(x), x \in \mathbb{R}^d\}$ is a GP, $E(f(x)) = m(x)$ and

$$Cov[f(x), f(x')] = E[\{f(x) - m(x)\} \{f(x') - m(x')\}] = k(x, x'). \tag{13}$$

Now assume the model of the form:

$$h(x)^T \beta, \tag{14}$$

where $f(X) \sim GP(0, K(x, x'))$. $f(x)$ are from a zero mean GP with covariance function $k(x, x')$. $h(x)$ are a set of basis functions that transform the original feature vector x in \mathbb{R}^d into a new vector x in \mathbb{R}^p . β is a $p - by - 1$ vector of basis function coefficients. An example of response y can be modeled as $P(y_i | f(x_i), x_i) \sim N(y_i | h(x_i)^T \beta + f(x_i), \sigma^2)$. Thus, a GPR model is a probabilistic model. A latent function $f(x_i)$ is introduced for each observation x_i , which makes the GPR model non-parametric. In vector form, the model is equivalent to

$$P(y | f, X) \sim N(y | H\beta + f, \sigma^2 I), \tag{15}$$

where

$$X = \begin{pmatrix} x_1^T \\ x_2^T \\ \vdots \\ x_n^T \end{pmatrix}, y = \begin{pmatrix} y_1 \\ y_2 \\ \vdots \\ y_n \end{pmatrix}, H = \begin{pmatrix} h(x_1^T) \\ h(x_2^T) \\ \vdots \\ h(x_n^T) \end{pmatrix}, f = \begin{pmatrix} f(x_1) \\ f(x_2) \\ \vdots \\ f(x_n) \end{pmatrix}. \tag{16}$$

The joint distribution of latent functions $f(x_1), f(x_2), \dots, f(x_n)$ in the GRP model is as follows:

$$P(f | X) \sim N(f | 0, K(X, X)). \tag{17}$$

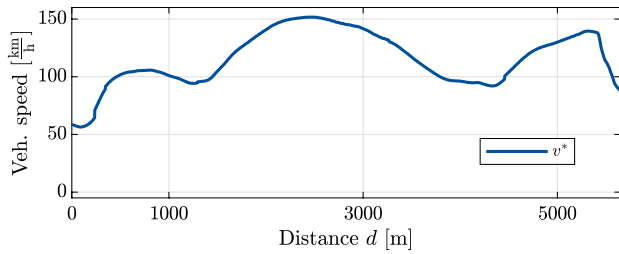


Fig. 2 Vehicle speed profile

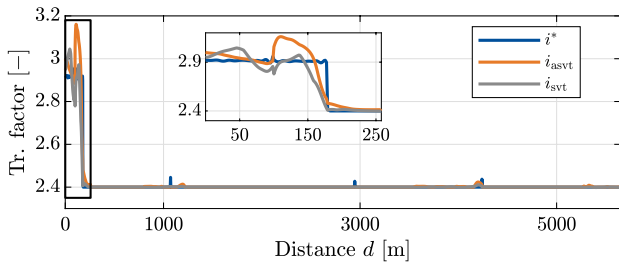


Fig. 3 Transmission factor prediction and measurement

For the covariance function $k(x, x')$ an ARD squared exponential [17] with separate length scales for each predictor [18] is used.

The GPR Model was trained by the same identification data set as the polynomial model proposed in [12] which contained 83% of the driving sequences in the data set. Inputs of the GPR are the electric motor's torque $T_{EM,k}$ the vehicle's speed \bar{v}_k and the battery's SOC $s_{c,k}$.

Results

To assess the presented approaches, the same data set is used as presented in [12]. The computational performance of the prediction is tested on an Intel Core i5-7600 CPU with 3.5 GHz. To validate the subsystems, a 6-fold cross validation is performed by splitting the data set into 6 separate parts. 5 of these parts are used to train the systems, while the remaining part is preserved for the validation. In Fig. 2, the speed profile of one validation drive sequence is shown.

Transmission Factor

In Fig. 3, the transmission factor prediction is shown. Here, i_{svt} is the predicted value using the approach presented in [12], while i_{asvt} is predicted using proposed approach of including additional acceleration input values, as defined in (5). The predictions are compared to the actual transmission factor i^* which can be calculated based on measured rotational drive shaft speed data, using equation (3). The

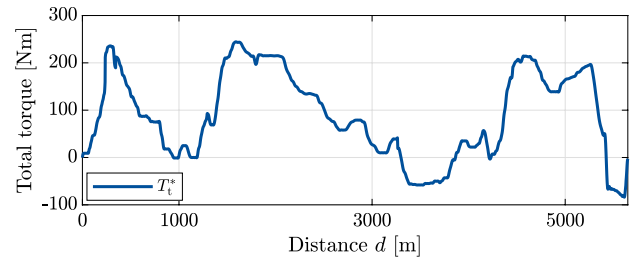


Fig. 4 Total driveshaft torque measurement

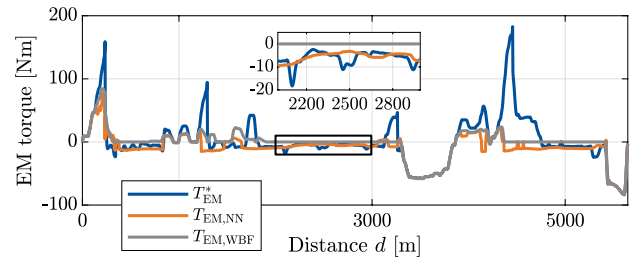


Fig. 5 Electric motor torque prediction and measurement

average root mean square error of the transmission model that additionally uses acceleration inputs results to 0.4263. Compared to the previous rmse of 0.407, a slight decrease in accuracy can be observed.

An additional effect of the added dimension is the increase in prediction time from 8 to 23 μ s. Hence, the additional consideration of the acceleration is not beneficial for the transmission factor prediction and is not further considered.

Torque Distribution

To evaluate the torque distribution model, the predicted torque of the combustion engine and the electric motor is compared with the measured CAN data. The averaged root mean square error results in 19.01 Nm for the combustion engine torque in a range of 0 Nm to 250 Nm. For the electric motor torque in 19.11 Nm in a range of -330 Nm to 330 Nm. The previous rmse is 17.33 Nm for the combustion engine torque and 23.11 Nm for the electric motor torque. Compared with another, the combustion engine's rmse increased, while the electric motor's rmse decreased. Figure 4 shows the total driveshaft torque T_t of the validation sequence.

Figure 6 shows the prediction of the combustion engine torque using the neural network approach $T_{CE,NN}$ and the prediction using weighted basis function $T_{CE,WBF}$. Figure 5 shows the prediction of the electric motor torque using the neural network approach $T_{EM,NN}$ and the prediction using the weighted basis function approach $T_{EM,WBF}$. Each figure compares the prediction with their measured equivalent $T_{CE,k}^*$ and $T_{EM,k}^*$. The predictions show a reasonable, overall fit. The

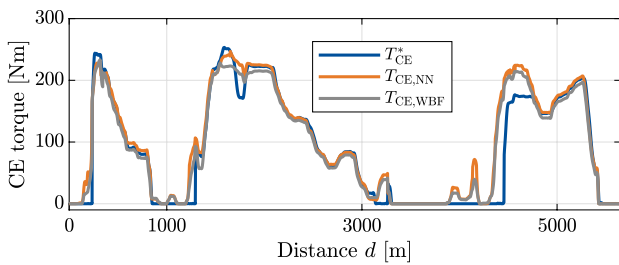


Fig. 6 Combustion engine torque prediction and measurement

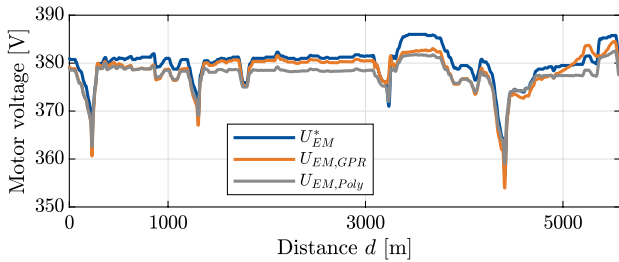


Fig. 7 Motor voltage prediction and measurement

combustion engines torque deviates just slightly, while the engine is running and the predicted electric motor torque shows a better fit during the load point adjustment, as shown in Fig. 5.

The extra torque required by the electric motor at the starting phases of the combustion engine can still not be met, as indicated by the positions 230 m, 1300 m and 4450 m. Furthermore, both torque distribution model indicate inaccuracies when predicting the combustion engine torque between 3900 m and 4150 m.

Even if the rmse of the combustion engine torque is higher than before, the increasing accurate of the electric motor torque prediction is beneficial, as the SOC is predicted based on this value [12]. The predicted SOC values are used in the transmission model as well as in the torque distribution model, which recursively affect the predictions in the following steps. Therefore, a more accurate prediction of the electric motor torque has a greater effect on the overall accuracy of the energy demand model.

Motor Voltage

The predicted motor voltage U_{EM} is evaluated based on the measured electric motor torque $T_{EM,k}^*$, the vehicle's speed \bar{v}_k^* and the battery's SOC $s_{c,k}^*$. Figure 7 illustrates the measured motor voltage U_{EM}^* , the voltage predicted by the GPR $U_{EM,GPR}$ and the voltage predicted by the polynomial model $U_{EM,Poly}$. It is noticeable that the curve of $U_{EM,GPR}$ follows the curve of the measured voltage better. The voltage rmse

results to 1.211 V compared to the former 1.738 V in a value range of 320–400 V. The GPR model returns a clearly better result for the motor voltage but indicated by a 30% decrease of the prediction error. However, it leads to a significant increase of prediction time. While the polynomial model needed 0.266 ns to compute a single prediction, the GPR model needed 5.464 ms. To further use the GRP model in the application it needs to be reviewed if the increased prediction time is acceptable to increase the accuracy of the energy demand prediction or if the time loss is too significant.

Conclusion

In this paper, several data-based approaches have been introduced to further improve an energy demand prediction model for a hybrid electrical vehicle, based on route data and speed values, proposed in [12]. In particular, the improvement of the prediction of the transmission factor, the torque distribution and the motor voltage was addressed. A data set of 525 driven kilometers was used to identify and validate the advanced prediction approaches on a Volkswagen VII GTE. The data set contains drive sequences of distances between 5 and 7 km.

The model to predict the transmission factor was expanded to 3 inputs to investigate the effect of an additional consideration of the acceleration. This expansion resulted in an increase of the prediction error by 4.7%.

To consider the load point adjustment of the hybrid electrical drive train, the torque distribution ratio is estimated by a feed-forward neural network, based on the total drive torque, the vehicle speed and the previous state of charge. Here, the prediction error for the combustion engine torque increased by 9.7% while the prediction error of the electric motor torque decreased 17.3%.

For the electric part of the powertrain, the motor voltage was estimated by an polynomial equation in [12], based on the electric motor torque and the battery's state of charge. In this work, a Gaussian process regression model that led to a minor root mean square error of 1.211 V was additionally presented. While the prediction accuracy of new model increased by 50%, the computation time increased by roughly twenty thousand times. Hence, a practical use of the new model is not guaranteed.

The prediction inaccuracies of the single powertrain components have been improved. In addition, future work will investigate approaches to enhance the prediction of other powertrain components. In addition, it is investigated how proposed improvement affect the corresponding state of charge prediction.

Author Contributions The authors contributed equally to this work.

Funding Open Access funding enabled and organized by Projekt DEAL. The underlying project of this study was funded by IAV GmbH, Berlin, Germany.

Availability of data The used data set will not be published.

Code availability The used source code will not be published.

Declarations

Conflict of interest The authors declare that they have no conflict of interest.

Ethics approval Not applicable.

Consent to participate Not applicable.

Consent for publication Not applicable.

Open Access This article is licensed under a Creative Commons Attribution 4.0 International License, which permits use, sharing, adaptation, distribution and reproduction in any medium or format, as long as you give appropriate credit to the original author(s) and the source, provide a link to the Creative Commons licence, and indicate if changes were made. The images or other third party material in this article are included in the article's Creative Commons licence, unless indicated otherwise in a credit line to the material. If material is not included in the article's Creative Commons licence and your intended use is not permitted by statutory regulation or exceeds the permitted use, you will need to obtain permission directly from the copyright holder. To view a copy of this licence, visit <http://creativecommons.org/licenses/by/4.0/>.

References

1. Radke T. Energieoptimale Längsführung Von Kraftfahrzeugen Durch Einsatz Vorausschauender Fahrstrategien, p. 217. KIT Scientific Publishing, Karlsruhe. 2013. <https://doi.org/10.5445/KSP/1000035819>.
2. Fink D, Czarnecki J-D, Wielitzka M, Schweers C, Trabelsi A. Fahrstilanalyse zur Erhöhung der Nutzerakzeptanz automatisiert energieeffizienter fahrzeu glängsführung. In: Digital-Fachtagung VDI MECHATRONIK. 2021;158–163. <https://doi.org/10.26083/TUPRINTS-0001762>.
3. Fink D, Dues T, Kortmann K-P, Blum P, Schweers C, Trabelsi A. A recursive gaussian process based online driving style analysis. In: 2023 American Control Conference (ACC), pp. 3187–3192. IEEE. <https://doi.org/10.23919/ACC55779.2023.1015649>.
4. Rosenzweig J, Bartl M. A review and analysis of literature on autonomous driving. Making Innov. 2015;1–57.
5. Bellman RE. Dynamic programming. Dover Publications, Mineola. 2003. <http://www.loc.gov/catdir/description/dover032/2002072879.html>.
6. Sajadi-Alamdari SA, Voos H, Darouach M. Ecological advanced driver assistance system for optimal energy management in electric vehicles. IEEE Intell Transp Syst Mag. 2020;92–109. <https://doi.org/10.1109/MITS.2018.2880261>.
7. Fiori C, Ahn K, Rakha HA. Microscopic series plug-in hybrid electric vehicle energy consumption model: Model development and validation. Transp Res Part D: Transp Environ. 2018;63:175–85. <https://doi.org/10.1016/j.trd.2018.04.022>.
8. Zhang F, Wang L, Coskun S, Pang H, Cui Y, Xi J. Energy management strategies for hybrid electric vehicles: review, classification, comparison, and outlook. Energies. 2020;13(13):3352. <https://doi.org/10.3390/en13133352>.
9. Zhang H, Cao D, Du H. Energy management of hybrid electric vehicles. In: Modeling, Dynamics and Control of Electrified Vehicles, pp. 159–206. Woodhead Publishing. 2018.
10. Hülsebusch D. Fahrerassistenzsysteme zur energieeffizienten Längsregelung - Analyse und Optimierung der Fahrsicherheit. KIT Scientific Publishing.
11. Pitanuwat S, Aoki H, Iizuka S, Morikawa T. Development of hybrid vehicle energy consumption model for transportation applications-part ii: traction force-speed based energy consumption modeling. World Electr Veh J. 2019;10(2):22.
12. Fink D, Shugar S, Ziaukas Z, Schweers C, Trabelsi A, Jacob H-G. Energy demand prediction in hybrid electrical vehicles for speed optimization. In: Proceedings of the 8th International Conference on Vehicle Technology and Intelligent Transport Systems (VEHITS 2022), 116–123. 2022. <https://doi.org/10.5220/001107560000319>.
13. Mitschke M, Wallentowitz H (eds.) Dynamik der Kraftfahrzeuge, Vierte, neubearbeitete auflage edn. VDI-Buch. Springer Berlin Heidelberg, Berlin, Heidelberg and s.l. 2004. <https://doi.org/10.1007/978-3-662-06802-1>.
14. Fink D, Schulz Y, Ziaukas Z, Schweers C, Trabelsi A, Jacob H-G. Assessment of algorithms for a real-time optimization of the vehicle speed. In: Proceedings of the 15th International Symposium on Advanced Vehicle Technology (AVEC '22), 2022.
15. Nelles O. Nonlinear system identification. Cham: Springer; 2020. <https://doi.org/10.1007/978-3-030-47439-3>.
16. Bianchini M, Maggini M, Jain LC (eds.) Handbook on neural information processing. In: Intelligent systems reference library, vol. Vol. 49. Springer, Berlin and Heidelberg, Monica. 2013.
17. Rasmussen CE. Gaussian processes in machine learning. Berlin, Heidelberg: Springer; 2004. https://doi.org/10.1007/978-3-540-28650-9_4.
18. Radford M, Neal S, Bickel P, Diggle P, Fienberg S, Krickeberg K, Olkin I, Wermuth NZ. Bayesian learning for neural networks vol. 118. Springer New York, New York, NY. 1996. <https://doi.org/10.1007/978-1-4612-0745-0>.

Publisher's Note Springer Nature remains neutral with regard to jurisdictional claims in published maps and institutional affiliations.